Changes in extreme Integrated water Vapor Transport on the U.S. west coast in NA-CORDEX, and relationship to mountain and inland precipitation

Mimi Hughes (mimi.hughes@noaa.gov)
NOAA Physical Sciences Laboratory https://orcid.org/0000-0003-0070-1512
Dustin Swales
NOAA Physical Sciences Laboratory
James D. Scott
NOAA Physical Sciences Laboratory
Michael Alexander
NOAA Physical Sciences Laboratory
Kelly Mahoney
NOAA Physical Sciences Laboratory
Rachel R McCrary
National Center for Atmospheric Research
Robert Cifelli
NOAA Physical Sciences Laboratory
Melissa Bukovsky
National Center for Atmospheric Research

Research Article

Keywords: mountain precipitation, regional climate change, atmospheric rivers

Posted Date: May 7th, 2021

DOI: https://doi.org/10.21203/rs.3.rs-493528/v1

Abstract

Western U.S. (WUS) rainfall and snowpack vary greatly on interannual and decadal timescales. This combined with their importance to water resources makes future projections of these variables highly societally relevant. Previous studies have shown that precipitation events in the WUS are influenced by the timing, positioning, and duration of extreme integrated water vapor transport (IVT) events (e.g., atmospheric rivers) along the coast. We investigate end-of-21st-century projections of WUS precipitation and IVT in a collection of regional climate models (RCMs) from the North American Coordinated Regional Downscaling Experiment (NA-CORDEX).

Several of the NA-CORDEX RCMs project a decrease in cool season precipitation at high elevation (e.g., across the Sierra Nevada) with a corresponding increase in the Great Basin of the U.S. We explore the causes of this terrain-related precipitation change in a subset of the NA-CORDEX RCMs through an examination of IVT-events. Projected changes in frequency and duration of IVT-events depend on the event's extremity: By the end of the century extreme IVT-events increase in frequency whereas moderate IVT-events decrease in frequency. Furthermore, in the future, total precipitation across the WUS generally increases during extreme IVT-events, whereas total precipitation from moderate IVT-events decreases across higher elevations. Thus, we argue that the mean cool season precipitation decreases at high elevations and increases in the Great Basin are largely determined by changes in moderate IVT-events which are projected to be less frequent and bring less high-elevation precipitation.

Full Text

Due to technical limitations, full-text HTML conversion of this manuscript could not be completed. However, the manuscript can be downloaded and accessed as a PDF.

Figures

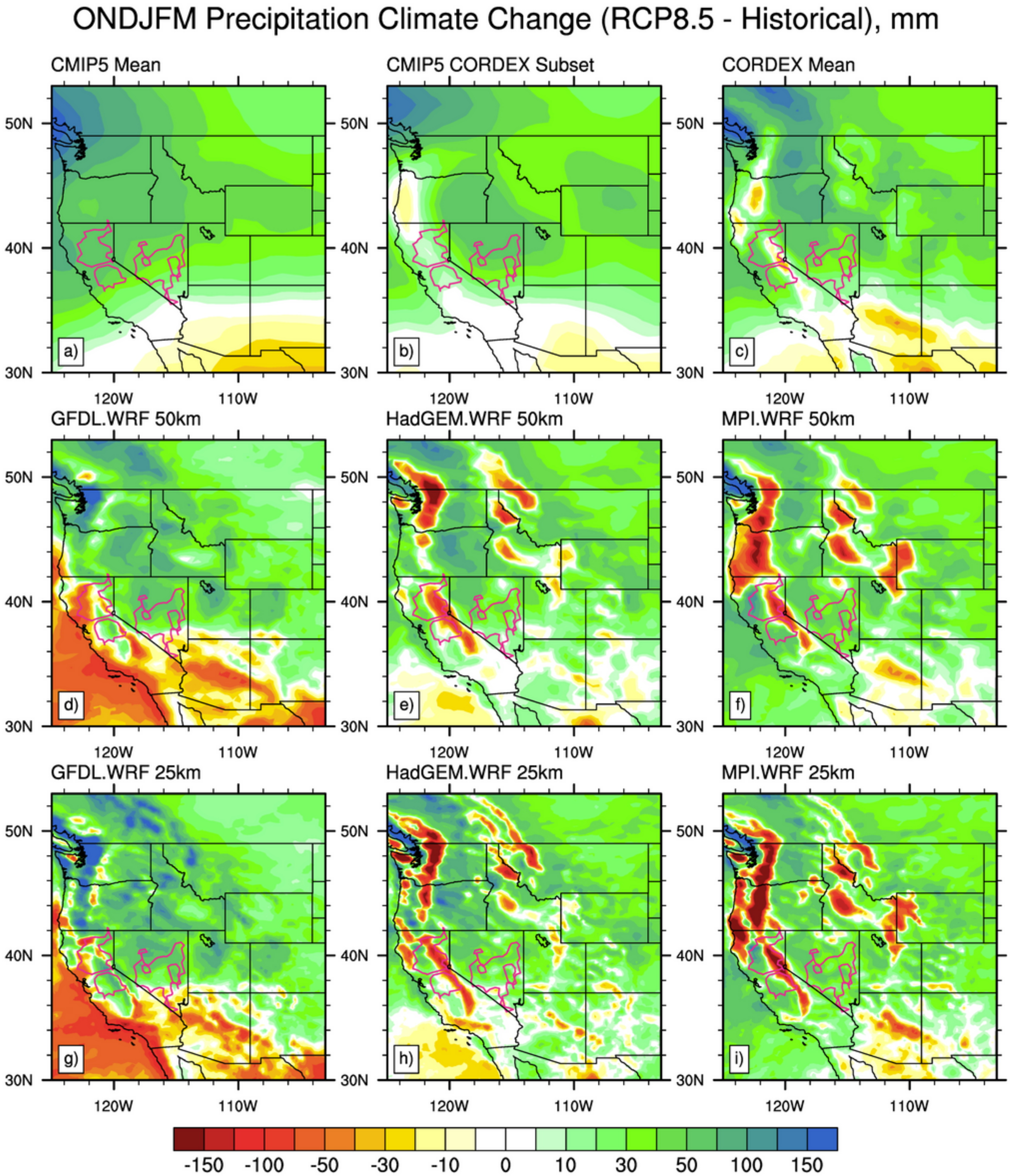

Figure 1

(a) Cool season total mean precipitation change in mm (RCP8.5 - historical) for CMIP5 ensemble. (b) Same as (a) except for five of six CMIP5 models used as boundary conditions for NA-CORDEX simulations (i.e., HADGEM2-ES, Can-ESM2, MPI-ESM-LR, MPI-ESM-MR, and GFDL-ESM2M). EC-EARTH is not included because no precipitation output was available. (c) Same as (a) but for NA-CORDEX ensemble. (d-f) Cool season total precipitation change in mm (RCP8.5 - historical) for 50 km (d)

GFDL.WRF, (e) HadGEM.WRF, and (f) MPI.WRF. (g-i) Cool season total precipitation change in mm (RCP8.5 - historical) for 25 km (g) GFDL.WRF, (h) HadGEM.WRF, and (i) MPI.WRF. Magenta contours outline three watersheds: Sacramento (top left), San Joaquin (bottom left), and Central Nevada River Basin (right).

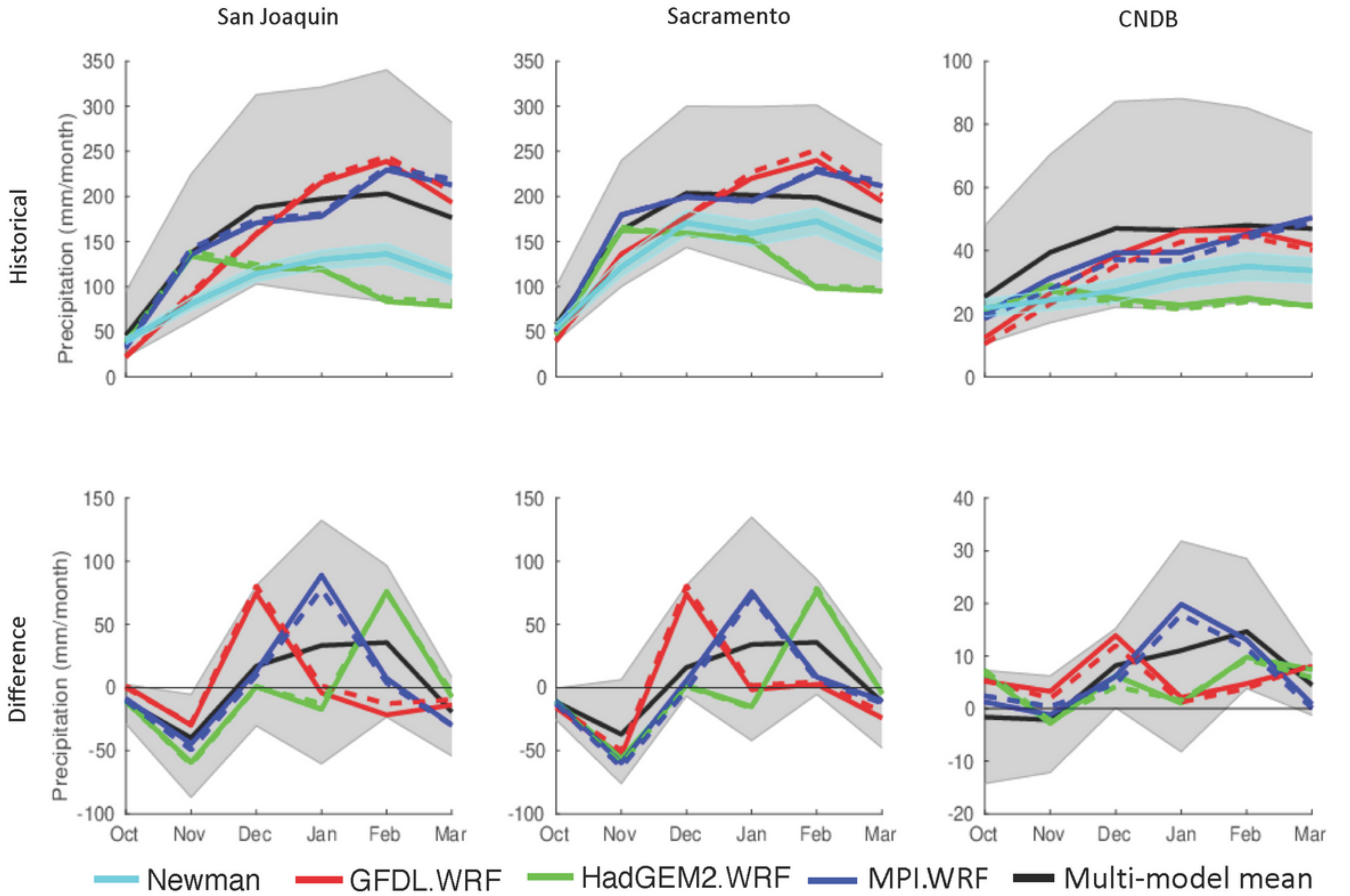

Figure 2

(top) Historical mean, and (bottom) difference (RCP8.5-historical) in monthly mean precipitation for (left) San Joaquin watershed, (middle) Sacramento watershed, and (right) CNDB watershed. Black line shows NA-CORDEX multi-model mean, and grey shaded region shows full range (minimum to maximum). Cyan line (shading) shows Newman mean (+/- 1 standard deviation). Red/green/blue lines show values from GFDL.WRF, HadGEM.WRF, and MPI.WRF, respectively, with solid lines for 50 km simulations and dashed lines for 25 km simulations. Locations of watersheds are shown on Figure 1. The y-axis range is much smaller for the CNDB.

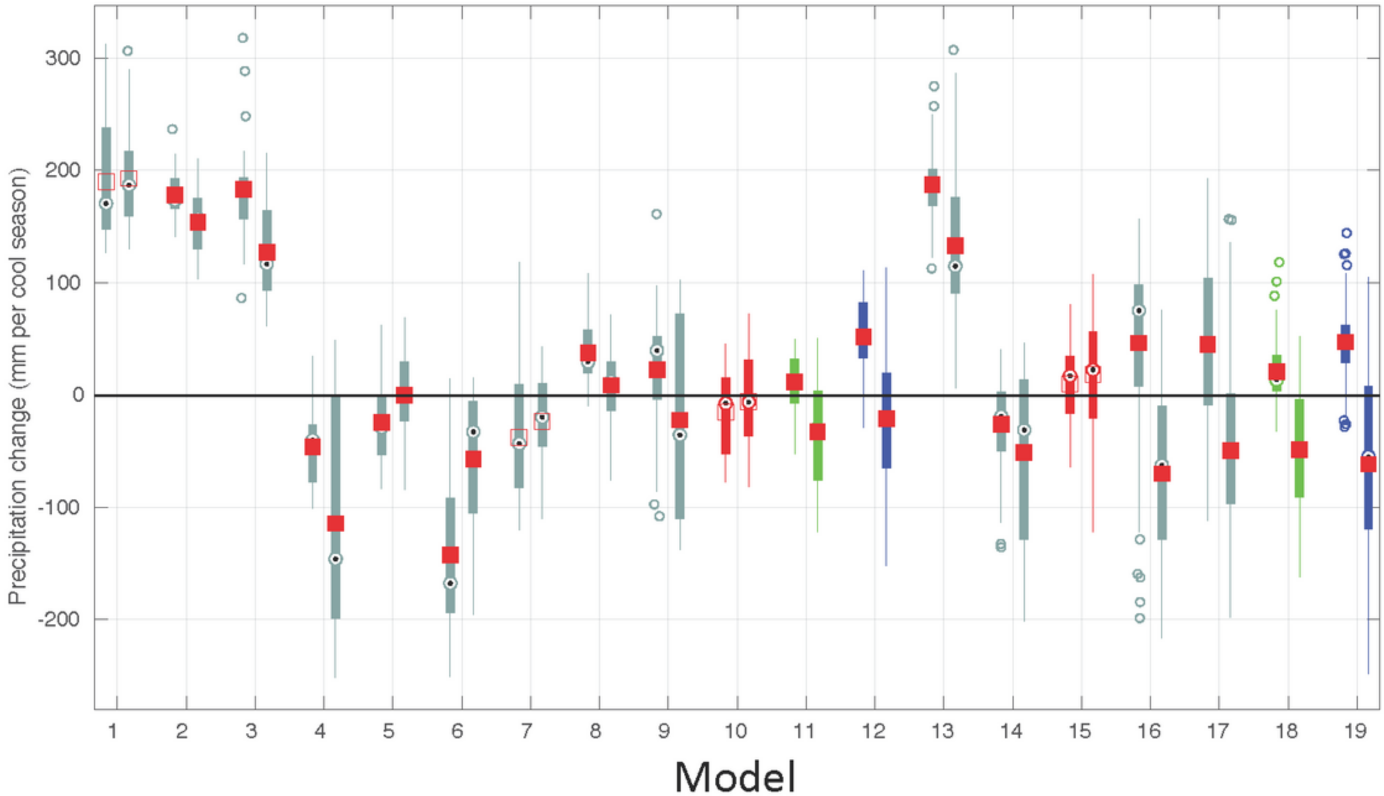

Figure 3

Total cool season precipitation changes for gridpoints in the two California watersheds for each NA-CORDEX model (labeled 1-19). Each model has two box/whisker plots: the left is gridpoints with elevations below 800 meters and the right is gridpoints with elevations above 800 meters. Open circles with black dots show median, boxes show 25/75 percentiles, whiskers extend to data points not considered outliers and small open circles show outliers. Red squares show means and are filled in for pairs that have significantly different means using a 2-sided t-test with 95% confidence intervals. Models 1-12 have ~50 km grid spacing and models 13-19 have ~25 grid spacing. Red, green, and blue bars show values from GFDL.WRF, HadGEM.WRF, and MPI.WRF, respectively.

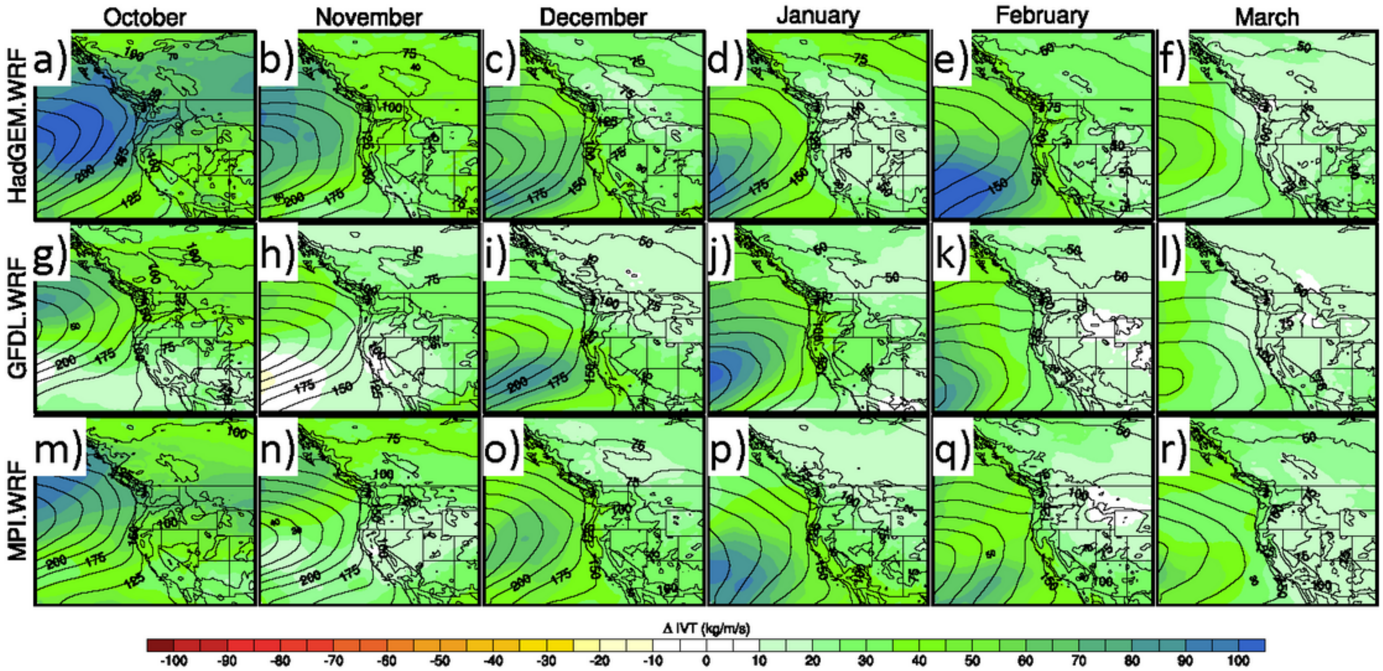

Figure 4

Change (RCP8.5-historical) in mean monthly IVT (color fill) for each cool season month (columns) and for each 25 km WRF simulation (rows). Historical IVT is shown in the black contours, contoured every 25 kg m-1 s-1.

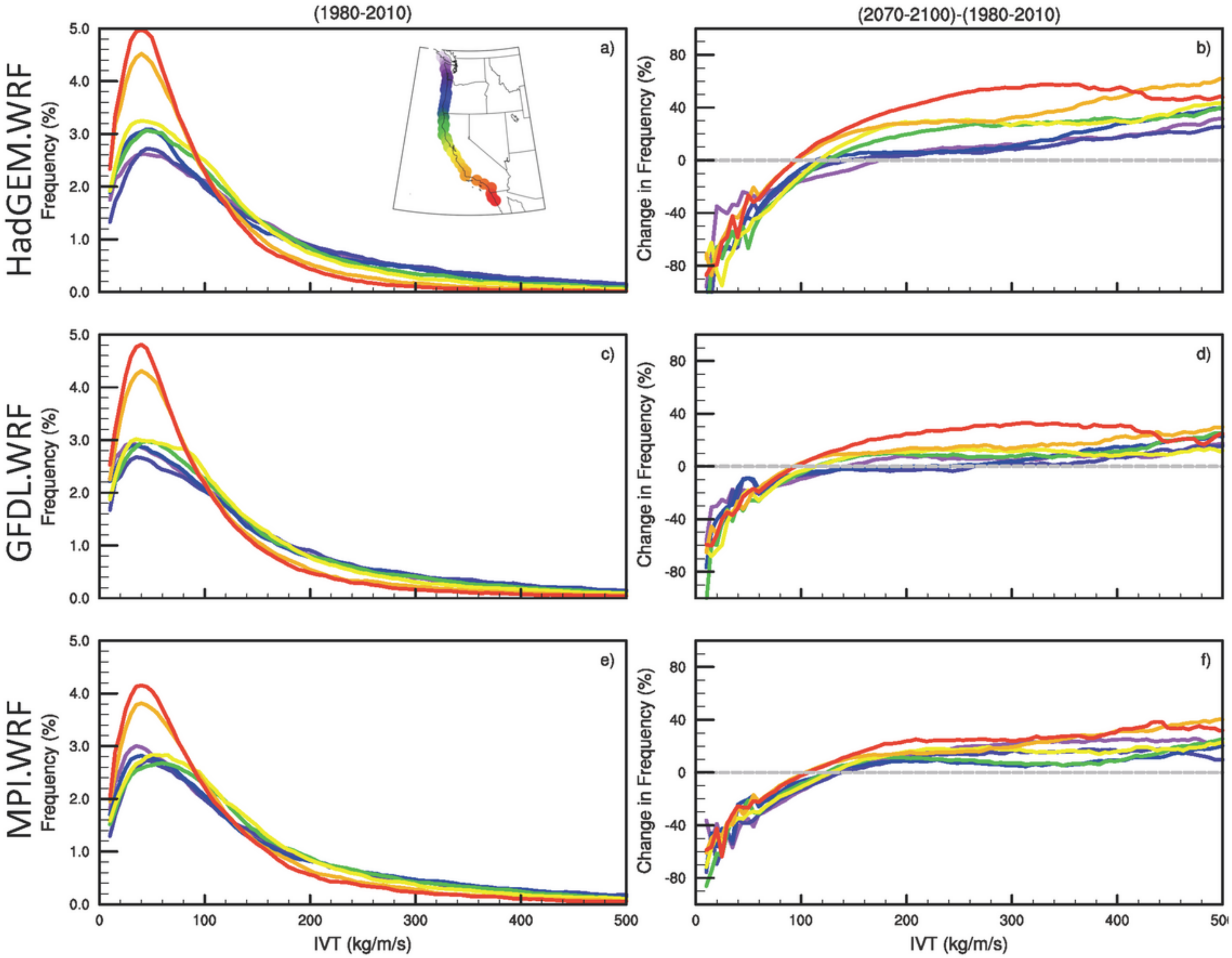

Figure 5

Estimated probability distribution functions (ePDF) of cool-season (ONDJFM) integrated water vapor transport (IVT) sampled every 3 hours at coastal locations (inset panel a) during: (a, c, e) historical and (b, d, f) difference (i.e., future-historical) in IVT ePDF, for (a, b) 25 km HadGEM.WRF, (c, d) 25 km MPI-ESM-LR.WRF, (e, f) 25 km GFDL.WRF. Inset in (a) shows locations of coastal gridpoints.

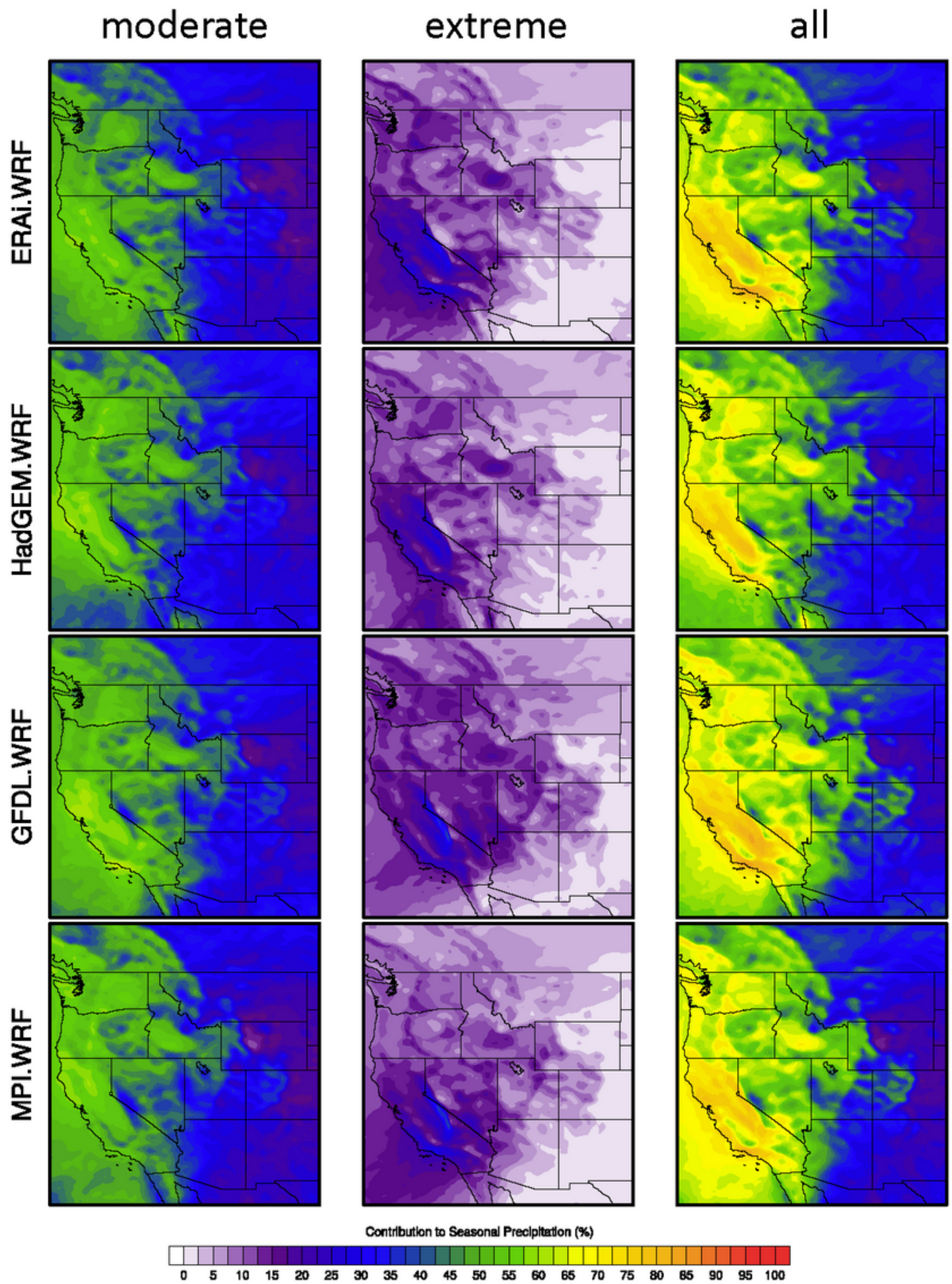

Figure 6

Contribution to cool season total precipitation associated with (left) moderate IVT events, (center) extreme IVT events, and (right) all IVT events in (top) ERAi.WRF, (second row) HadGEM.WRF, (third row) GFDL.WRF, and (bottom) MPI.WRF in 25 km WRF simulations.

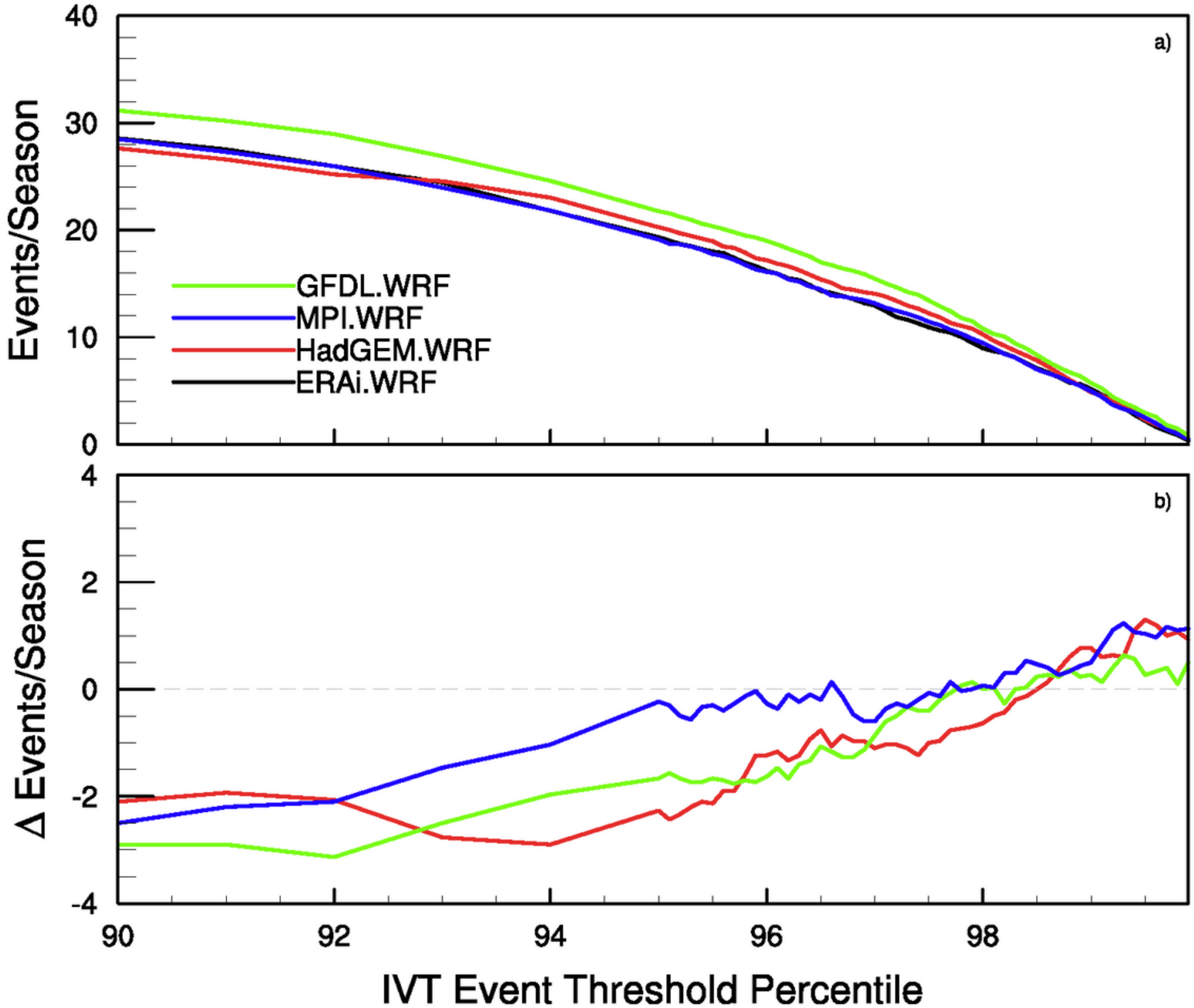

Figure 7

Cool-season (ONDJFM) 24-hour IVT event statistics for historical and future simulations for IVT events along entire western US coastline in 25 km WRF simulations, as a function of IVT event threshold percentile. (a) Historical IVT event statistics for GFDL.WRF, MPI.WRF, HadGEM.WRF, and ERA-I.WRF. (b) Future-Historical IVT event statistics.

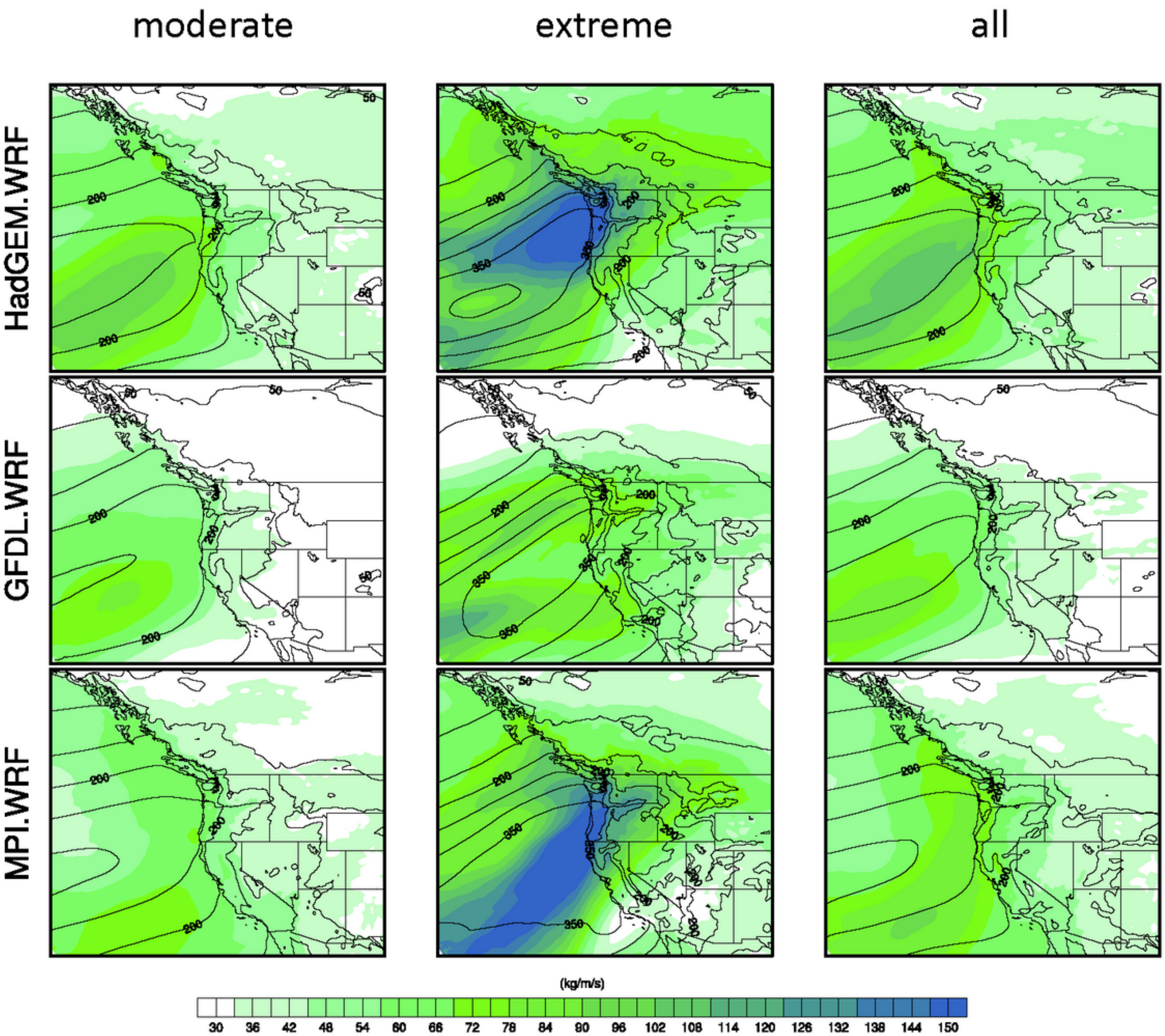

Figure 8

Change (future – historical, as color fill) in mean IVT during (left) moderate IVT events, (center) extreme IVT events, and (right) all IVT events in (top) HadGEM.WRF, (middle) GFDL.WRF, and (bottom) MPI.WRF in 25 km WRF simulations. Black contours show historical mean IVT event IVT contoured every 50 kg m-1 s-1.

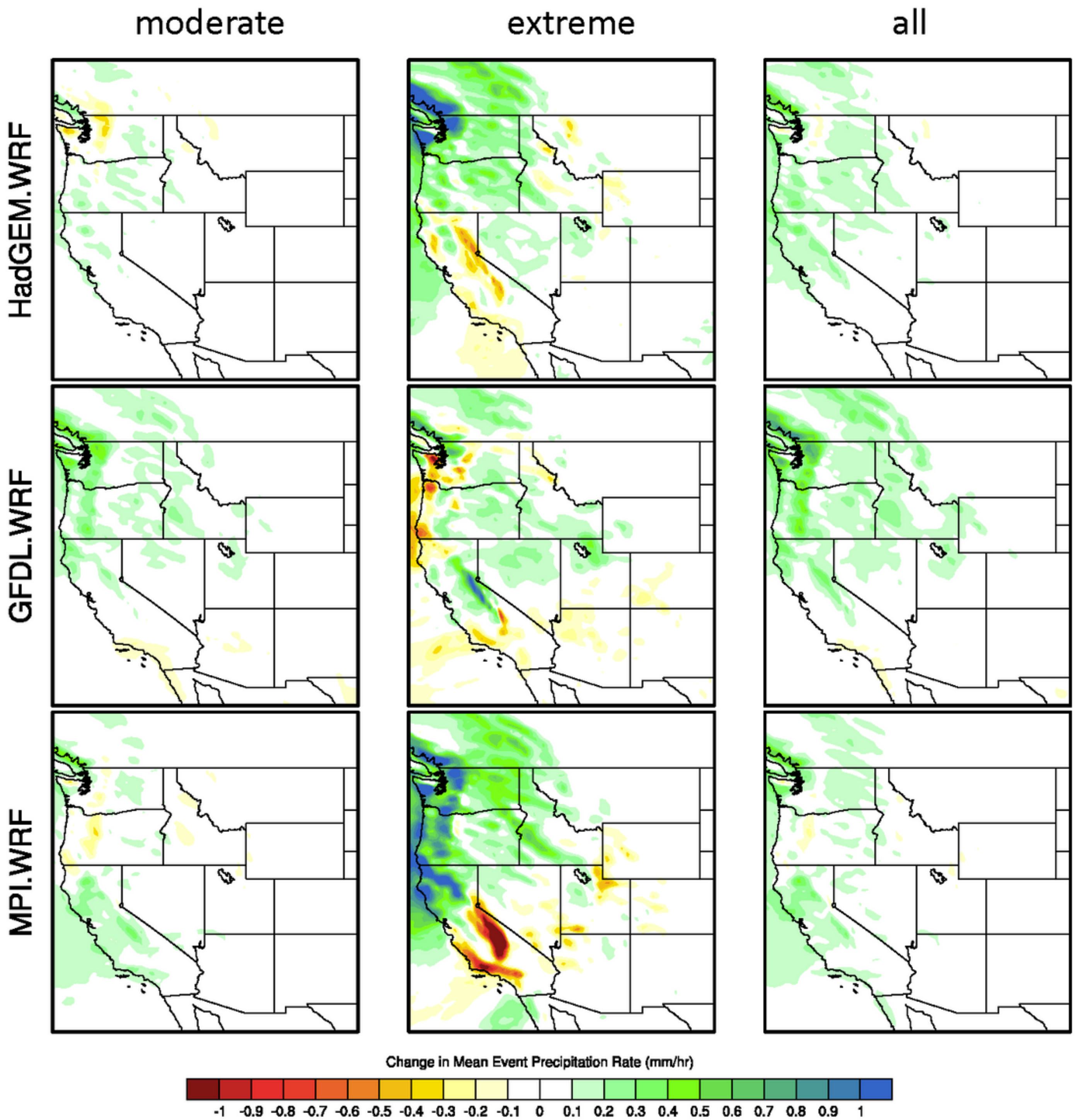

Figure 9

Change (future – historical) in mean precipitation rates during (left) moderate IVT events, (center) extreme IVT events, and (right) all IVT events in (top) HadGEM.WRF, (middle) GFDL.WRF, and (bottom) MPI.WRF in 25 km WRF simulations.

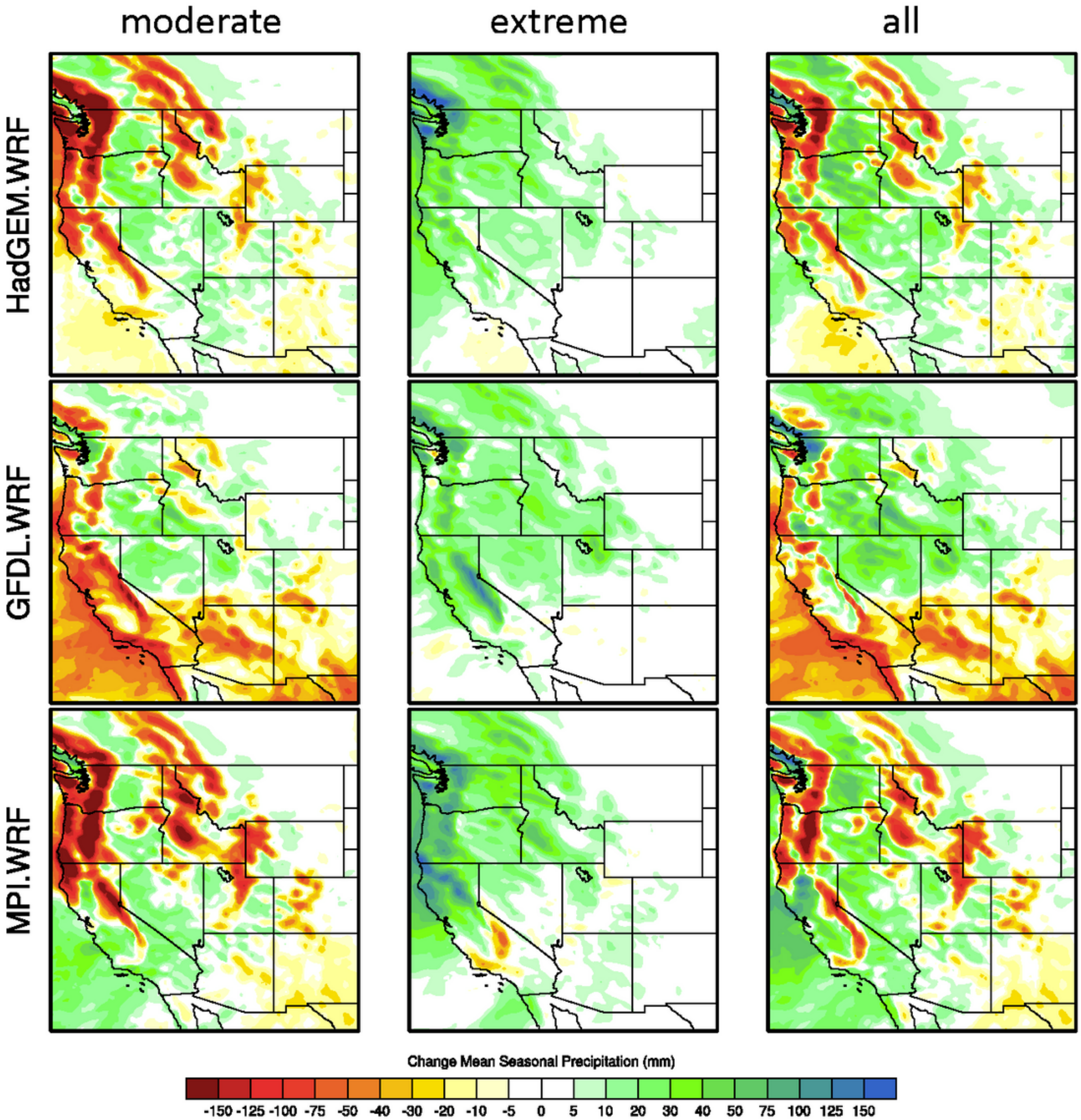

Figure 10

Change (future – historical) in mean seasonal precipitation from (left) moderate IVT events, (center) extreme IVT events, and (right) all IVT events in (top) HadGEM.WRF, (middle) GFDL.WRF, and (bottom) MPI.WRF in 25 km WRF simulations.

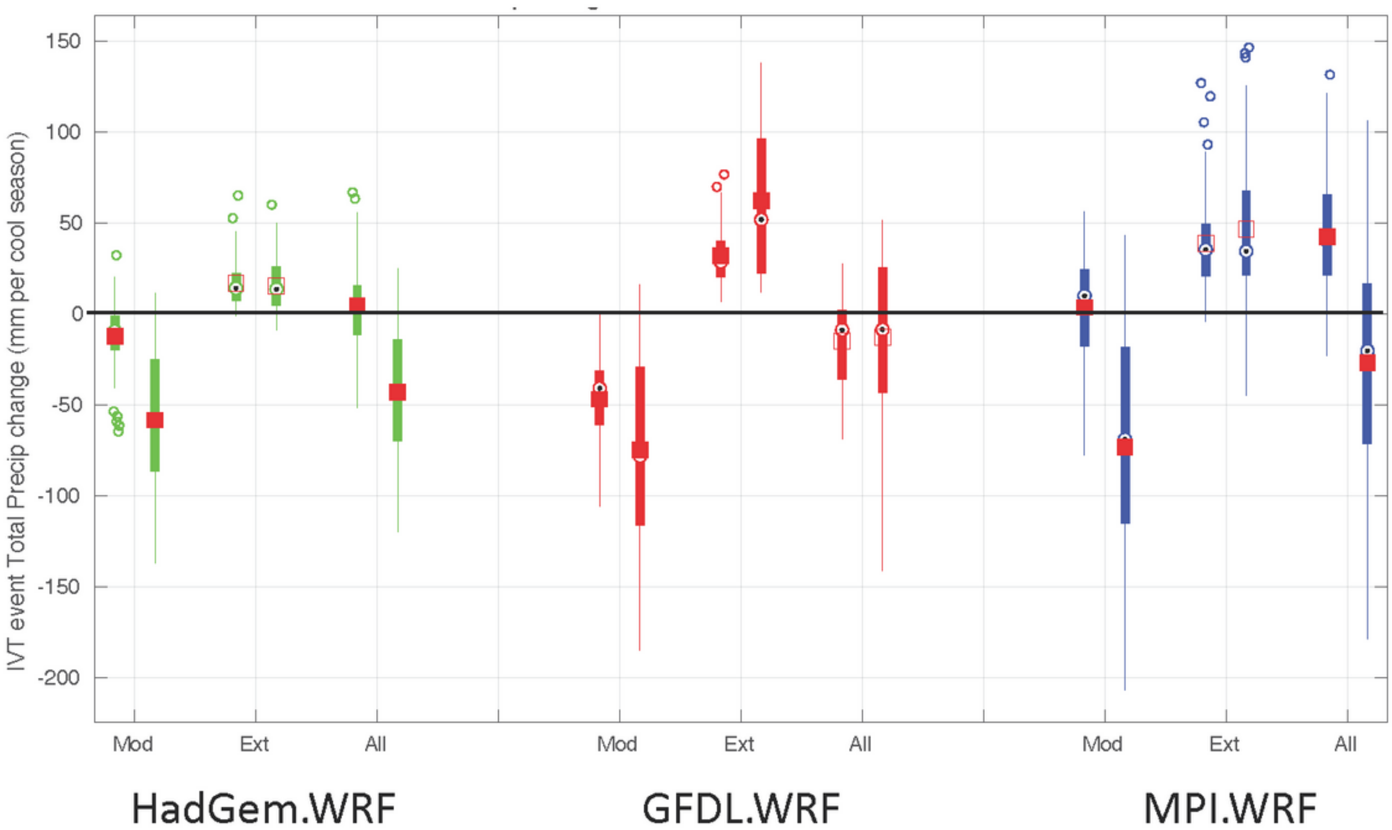

Figure 11

IVT event total precipitation changes (normalized to mm per cool season) in the two California watersheds for 25 km HadGEM.WRF, GFDL.WRF, and MPI.WRF (green, red, and blue box/whiskers, respectively). Each model has three pairs of two box/whisker plots, corresponding to the results for Moderate (left pair), Extreme (middle pair), and All (right pair) IVT events. As in Figure 3, the left in each pair is gridpoints with elevations below 800 meters and the right is gridpoints with elevations above 800 meters. Open circles with black dots show median, boxes show 25/75 percentiles, whiskers extend to data points not considered outliers and small open circles show outliers. Red squares show means and are filled in for pairs that have significantly different means using a 2-sided t-test with 95% confidence intervals.

Supplementary Files

This is a list of supplementary files associated with this preprint. Click to download.

- SupplementalMaterial.pdf